

# Immortalization of different breast epithelial cell types results in distinct mitochondrial mutagenesis.

Sujin Kwon<sup>1</sup>, Susan S. Kim<sup>3,4</sup>, Howard E. Nebeck<sup>1,4</sup>, Eun Hyun Ahn<sup>1,2,\*</sup>

<sup>1</sup>Department of Pathology, University of Washington, Seattle, WA 98195, USA; kwonsu17@uw.edu (S.J.K); henebeck@uw.edu (H.E.N); ahneun@uw.edu (E.H.A)

<sup>2</sup>Institute of Stem Cell and Regenerative Medicine, University of Washington, Seattle, WA 98109, USA; ahneun@uw.edu (E.H.A)

<sup>3</sup>Department of Biochemistry, University of Washington, Seattle, WA 98195, USA; ssk773@uw.edu (S.S.K)

<sup>4</sup>Equal contribution

\* Correspondence to: ahneun@uw.edu

Received: date; Accepted: date; Published: date

**Abstract:** Different phenotypes of normal cells might influence genetic profiles, epigenetic profiles, and tumorigenicities of their transformed derivatives. In this study, we investigated whether the whole mitochondrial genome of immortalized cells can be attributed to different phenotypes (stem vs non-stem) of their normal epithelial cell originators. To accurately determine mutations, we employed Duplex Sequencing, which exhibits the lowest error rates among currently available DNA sequencing methods. Our results indicate that the vast majority of observed mutations of the whole mitochondrial DNA occur at low-frequency (rare mutations). The most prevalent rare mutation types are C→T/G→A and A→G/T→C transitions. Frequencies and spectra of homoplasmic point mutations are virtually identical between stem cell-derived immortalized (SV1) cells and non-stem cell-derived immortalized (SV22) cells, verifying that both cell types were derived from the same woman. However, frequencies of rare point mutations are significantly lower in SV1 cells ( $5.79 \times 10^{-5}$ ) than in SV22 cells ( $1.16 \times 10^{-4}$ ). Additionally, the predicted pathogenicity for rare mutations in the mitochondrial tRNA genes is significantly lower (by 2.5-fold) in SV1 cells than in SV22 cells. Our findings suggest that the immortalization of normal cells with stem cell features leads to decreased mitochondrial mutagenesis, particularly in noncoding RNA regions. The mutation spectra and mutations specific to stem cell-derived immortalized cells (vs non-stem cell derived) have implications in characterizing heterogeneity of tumors and understanding the role of mitochondrial mutations in immortalization and transformation of human cells.

**Keywords:** Mitochondrial DNA, rare mutation, stem cells, breast cancer, tRNA, Duplex Sequencing, next generation sequencing

---

## 1. Introduction

Evidence exists that distinct phenotypes of normal cell [1-5] or precancerous cell [6] originators for tumor derivatives lead to tumor heterogeneities. For example, Ince et al (2007) reported that breast tumorigenic cells transformed from two different normal epithelial cell types (BPECs; HMECs) exhibited marked differences in histopathology, tumorigenicity, and metastatic abilities. Transformed BPECs caused lung metastases, whereas transformed HMECs were nonmetastatic [4]. Transformed BPECs were up to 104-fold more tumorigenic than transformed HMECs. However, no study has investigated subclonal mutations for transformed derivatives of different normal cell types.

Here, to study consequences of normal cell origins on genetic changes in their immortalized derivatives, we examined two different immortalized (pre-neoplastic) breast epithelial cell types that

46 were derived from normal human breast epithelial cells (HBECs) with different phenotypes (Types I  
47 and II). Both Type I and Type II normal HBECs were isolated from breast tissue of the same woman;  
48 however, they exhibited different phenotypes. Type I HBECs display stem cell characteristics and  
49 have been characterized by: the expression of a stem cell marker octamer-binding transcription  
50 factor 4 (Oct-4) [7] and estrogen receptor (ER)- $\alpha$  [8], and luminal epithelial markers [9,10]; a  
51 deficiency in gap-junction associated intercellular communication (GJIC) [9,11]; the ability to  
52 display anchorage-independent growth [11]; the ability to differentiate into Type II (normal  
53 differentiated) HBECs [9,11]; reduced expression of maspin [12]; and the ability to form  
54 budding/ductal organoids on Matrigel in conjunction with Type II HBECs [11]. In contrast, Type II  
55 HBECs exhibit opposite phenotypes in the described features above (i.e., do not express stem cell  
56 markers; do not express ER- $\alpha$ ; express basal epithelial markers; express GJIC proteins; higher  
57 expression of maspin).

58 Both Type I (stem cell features) and Type II (without stem cell features) HBECs were  
59 transformed with Simian virus 40 large T-antigen (SV40-T) into immortal/non-tumorigenic  
60 (pre-neoplastic) cells, M13SV1 and M13SV22, respectively. SV40-T is widely used to immortalize  
61 and transform mammalian cells [13,14]. Type II HBECs are less susceptible to SV40-T  
62 transformation than are Type I HBECs, and rarely become immortal following transfection with  
63 SV40-T [8,9,11,15]. This suggests that Type I HBECs and Type I HBEC-derived immortalized cells  
64 appear to be the major target cells for breast carcinogenesis and transformation.

65 In the present study, we examined whether the whole mitochondrial genome of these different  
66 immortalized human breast epithelial cell types is influenced by phenotypes of their originator  
67 normal HBECs (Type I and Type II). To accurately investigate low-frequency (heteroplasmic) rare  
68 and subclonal mutations as well as high-frequency (homoplasmic) mutations, we applied Duplex  
69 Sequencing (DS), which detects mutations with unprecedented accuracy [16-19]. Unlike  
70 conventional sequencing technologies that sequence only a single strand of DNA, DS sequences both  
71 strands of DNA and scores mutations only if they are present in both strands of the same DNA  
72 molecule as complementary substitutions. This significantly lowers background error rates (eg.,  
73 Next generation sequencing error rates  $10^{-2}$  to  $10^{-3}$ ; DS error rates  $< 5 \times 10^{-8}$ ) [16,17,19-21].

## 74 2. Results

75 In this study, non-stem cell-derived immortalized human breast epithelial cells (HBECs) will  
76 be referred to as SV22 and stem cell-derived immortalized HBECs will be referred to as SV1 cells.  
77 Both SV22 and SV1 cells were cultured under the same conditions, DNA was extracted, and DNA  
78 libraries were prepared for Duplex Sequencing (DS) as we have described previously [22]. The  
79 average number of nucleotides at each genome position (depth) was calculated as the total number  
80 of duplex consensus sequence (DCS) nucleotides sequenced divided by the mtDNA size of 16569  
81 bases. The DCS depths were 1060 (all Tables and Figures except Fig S4) for SV22 cells and 1666 (all  
82 Figures and Tables) and 2738 (Fig S4) for SV1 cells. These are estimated to be equivalent to  
83 single-strand tag-based sequencing depths of approximately 5000 to 6200 and 7900 to 9800,  
84 respectively [19].

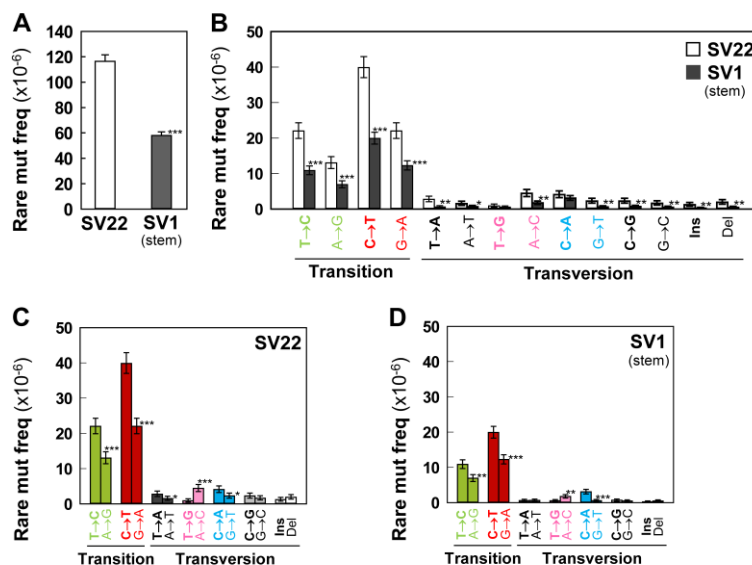
85 We have defined mtDNA mutations (variants) found in SV22 and SV1 cells as homoplasmic  
86 (90-100%), subclonal (0-10%) and rare (0-1%) based on the mutation occurrence (%) at each genome  
87 position. Maternally inherited mitochondrial mutations arising during early embryonic  
88 development are more likely to be homoplasmic [23,24]. In the present study, we focused on rare  
89 and subclonal variants, as they presumably represent *de novo* somatic variants. Rare or subclonal  
90 mutations are not accurately determined by conventional sequencing methods due to their high  
91 background error frequencies ( $10^{-2}$  to  $10^{-3}$ ) [20,21,25]. These rare and subclonal mutations, however,  
92 are accurately detectable by Duplex Sequencing [16-19].

93 *2.1. Both SV22 and SV1 cells exhibit identical homoplasmic mutations, verifying that both cell types were*  
94 *derived from the same individual.*

95 Thirty-five identical homoplasmic unique mutations were found between the two cell types  
 96 (Fig S1). Frequencies, types (%), and context fractions (%) of homoplasmic mutations were almost  
 97 identical (Fig S1) in both cell types. T>C/A>G and C>T/G>A transitions are the only mutation types  
 98 observed with T>C/A>G being more dominant than C>T/G>A (Fig S1). As homoplasmic  
 99 mitochondrial mutations are more likely to be maternally inherited mutations or variants arising  
 100 during early embryonic development, our finding of identical homoplasmic mutations between the  
 101 two cell types verify that they were derived from the same woman.

102 2.2. SV1 cells show significantly lower frequencies of rare mutations and subclonal mutations than do SV22  
 103 cells.

104 We determined frequencies of rare and subclonal mutations in both cell types by Duplex  
 105 Sequencing. The overall frequencies of both rare (Fig 1A) and subclonal (Fig S2A) mutations are  
 106 significantly lower in SV1 cells (by 2-fold) than in SV22 cells. In addition, we determined frequencies  
 107 of each point mutation type, of insertions, and of deletions. C>T/G>A and T>C/A>G transitions are  
 108 the most dominant types for both cell types (Figs 1B-D, Figs S2B-D). Frequencies of each type of rare  
 109 and subclonal mutation are also significantly lower in SV1 cells than in SV22 cells (Figs 1B, S2B).



110

111 **Figure 1.** Frequencies of rare mutations in the whole mtDNA. Overall rare mutation frequency (A)  
 112 and frequencies of rare mutation types (B-D) for SV22 (immortalized non-stem) and SV1  
 113 (immortalized stem) cells were determined using Duplex Sequencing. Error bars represent the  
 114 Wilson Score 95% confidence intervals. Significant differences in rare mutation frequencies between  
 115 two groups are indicated (\* p < 0.05, \*\* p < 5 x 10<sup>-4</sup>, and \*\*\* p < 5 x 10<sup>-10</sup>) by the 2-sample test for  
 116 equality of proportions with continuity correction.

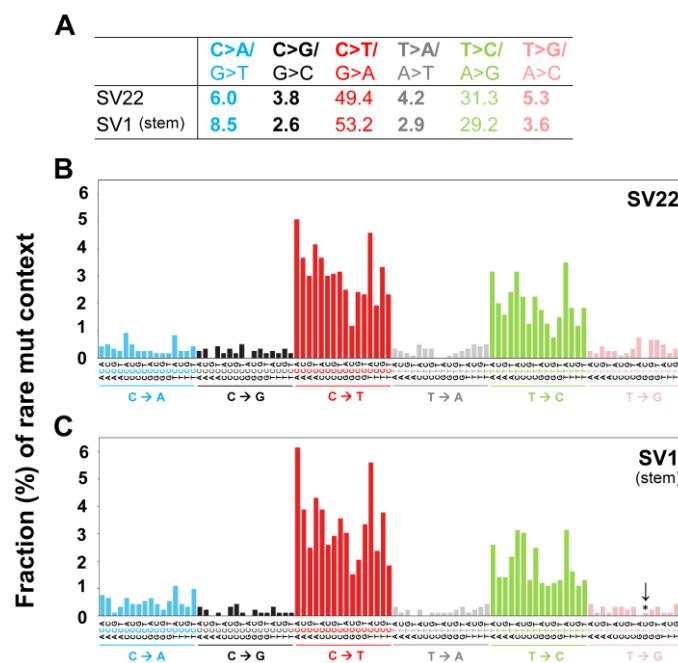
117 2.3. The strand bias of rare and subclonal mutations are observed in both cell types.

118 The two strands of mtDNA are designated as heavy (H) and light (L) strands [26]. Our DS data  
 119 are referenced to the L-strand. In the L-strand of both SV22 and SV1 cells, C>T are significantly  
 120 more prevalent than G>A; T>C are significantly more prevalent than A>G; A>C are significantly  
 121 more prevalent than T>G; C>A are significantly more prevalent than G>T (Figs 1C-D, S2C-D). These  
 122 significant asymmetric distributions within the complementary mutation type reflect a strand  
 123 orientation bias in both cell types.

124 2.4. C>T/G>A transitions are the most prevalent mutation types followed by T>C/A>G in both cell types.

125 The fraction (%) of rare and subclonal mutation types were calculated (Figs 2A, S3A). In both  
 126 SV22 (non-stem) and SV1 (stem) cells, the most prevalent rare and subclonal mutation types are  
 127 C>T/G>A and T>C/A>G (Figs 2A, S3A). The percentages of C>T/G>A and T>C/A>G rare mutations  
 128 are similar between both cell types. In contrast, the fractions of the four rare mutation types in SV22  
 129 and SV1 cells are different by about 1.5-fold with higher fractions C>G/G>C, T>A/A>T, and  
 130 T>G/A>C mutation types in SV22 cells and higher fractions of C>A/G>T mutation types in SV1 cells  
 131 (Fig 2A).

132 To investigate influences of neighboring bases on types of rare and subclonal mutations, the  
 133 bases immediately 5' and 3' to each mutated base were identified (i.e. the mutation occurs at the  
 134 second position of each such trinucleotide). This allows classification of observed substitutions into  
 135 96 categories (4 bases X 6 substitutions x 4 bases). Numbers and fractions (%) of these mutation  
 136 trinucleotides in each of the categories compose the "mutation context spectra" (MCS) of the cells.  
 137 For both rare and subclonal mutations, T>G transversions in context GTA were significantly lower  
 138 ( $p=0.02$ ) in SV1 than in SV22 cells (Figs 2B-C, S3B-C).



139

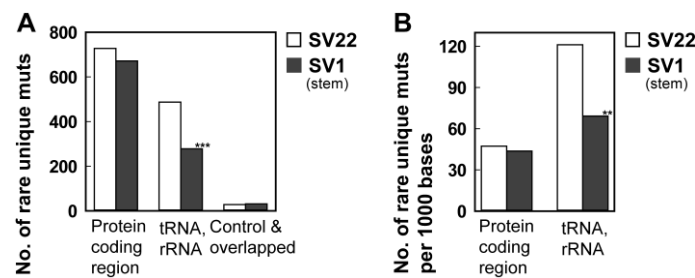
140 **Figure 2.** Types and sequence context spectra of rare unique mutations in the whole mtDNA.  
 141 Fractions (%) of rare mutation types (A) and fractions (%) of rare mutation context spectra (B,C) for  
 142 SV22 (immortalized non-stem) and SV1 (immortalized stem) cells were determined using Duplex  
 143 Sequencing. Trinucleotide contexts (B,C) are the mutated base surrounded by all possibilities for its  
 144 immediate 5' and 3' bases. To keep the graph concise, these point mutation trinucleotides are  
 145 complemented as necessary to always depict the reference base as the pyrimidine of its pair. The  
 146 fraction (%) of each specific trinucleotide out of all 96 possible trinucleotide contexts depicts the  
 147 contribution of each genome sequence context to each point mutation type. Significant differences in  
 148 fractions (%) of mutation context types between the two groups are indicated (\*  $p < 0.05$ ) by the  
 149 2-sample test for equality of proportions with continuity correction).

150 **2.5. The decreased mitochondrial mutagenesis of SV1 cells occurs mainly in the noncoding RNA region (rRNA**  
 151 **and tRNA) of the mitochondrial genome**

152 The human mitochondrial genome consists of three regions: protein coding (13 genes),  
 153 non-coding (nc) RNA (2 rRNA and 22 tRNA genes), and control/overlapped regions. We examined  
 154 which of the three regions is more vulnerable to mitochondrial mutagenesis (Fig 3A, Table S1) in  
 155 SV22 and SV1 cells.

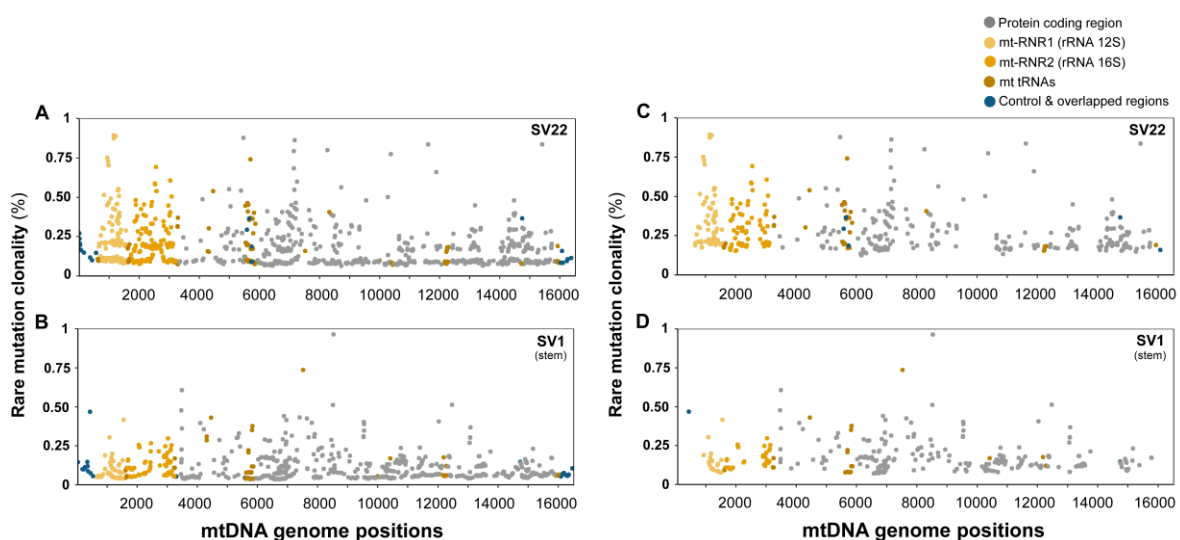
156 Of the three categorized regions, the ncRNA regions exhibit the most significant differences in  
 157 the number of rare mutations between SV22 and SV1 cells. The number of rare unique mutations in

158 the ncRNA regions is significantly lower in SV1 cells than in SV22 cells (Fig 3A, Table S1;  $p =$   
 159  $2.6 \times 10^{-15}$ ). However, the sizes of the three regions are different, contributing to a bias in the number  
 160 of observed unique mutations. In particular, the number of bases of the protein coding regions  
 161 (11341) is greater than that of the ncRNA (4020) and the control/overlapped regions (approximately  
 162 1772) [27]. Thus, to compare mutation prevalence per the same genome size between  
 163 protein-coding regions and ncRNA regions, we estimated the number of rare unique mutations per  
 164 1000 bases and found an even more significantly higher number of rare unique mutations in  
 165 ncRNA regions than in the protein coding regions. This indicates that the ncRNA regions are more  
 166 susceptible to mitochondrial mutagenesis than the protein-coding regions. Within the ncRNA  
 167 region itself, there is a significantly lower number of rare unique mutations in SV1 cells than in  
 168 SV22 cells (Fig 3B, Table S2;  $p = 1 \times 10^{-4}$ ). Genome position and clonality (%) for each of the rare  
 169 mutations observed in SV22 and SV1 cells are presented in Figure 4A,B. The average and median  
 170 clonalities (%) of rare mutations are still about 1.7-fold significantly lower in SV1 cells ( $0.17\% \pm$   
 171  $0.006$ ) (Fig 4D) than in SV22 cells ( $0.29\% \pm 0.007$ ) (Fig 4C), even after excluding variants that were  
 172 mutated only once (singlet mutations).



173

174 **Figure 3.** Number of rare unique mutations considered (individually and per 1000 bases) by genome  
 175 positional category in the whole mtDNA. Number of rare unique mutations by positional category  
 176 (A) and number of rare unique mutations per 1000 bases by positional category (B) were determined  
 177 using ANNOVAR for SV22 (immortalized non-stem) and SV1 (immortalized stem) cells. Significant  
 178 differences in numbers of rare mutations between the two groups are indicated (\*  $p < 0.05$ , \*\*  $p < 5 \times$   
 179  $10^{-4}$ , and \*\*\*  $p < 5 \times 10^{-10}$ ) by the 2-sample test for equality of proportions with continuity correction.



180

181

182 **Figure 4.** Genomic positions and clonalities (%) of rare unique mutations in the whole mtDNA. Rare  
 183 mutation clonalities (%) by genomic position including singlets (A,B) or excluding singlets (C,D)  
 184 were determined for SV22 (immortalized non-stem) and SV1 (immortalized stem) cells using Duplex  
 185 Sequencing. Singlets are defined as variants that are mutated only once in nucleotides sequenced at a  
 186 specific genome position.



187 2.6. Proportions (%) of nonsynonymous mutations in mitochondrial protein coding regions and their predicted  
188 pathogenicity scores of subclonal mutations are similar between SV22 and SV1 cells

189 We compared the proportion (%) of nonsynonymous mutations (causing changes in amino  
190 acids) of mitochondrial protein coding regions between SV22 and SV1 cells. Overall, no significant  
191 differences in rare or subclonal mutations were observed in the mitochondrial protein coding  
192 region between the two cell types (Table S3).

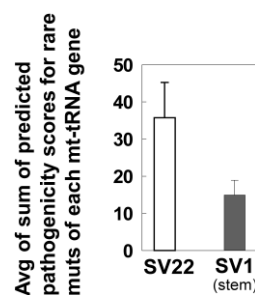
193 2.7. Predicted pathogenicity scores of missense mutations of mitochondrial protein coding regions are similar  
194 between SV22 and SV1 cells.

195 Predicted pathogenicity scores of the subclonal missense mutations were evaluated using  
196 MutPred [28]. MutPred provides a general  $g$  score for each missense mutation, where a higher  $g$   
197 score indicates a higher chance that an amino acid substitution is deleterious. The average of the  $g$   
198 score sums for each of the 13 mtDNA protein-coding genes was calculated for subclonal missense  
199 mutations present only in SV22 cells ( $4.25 \pm 0.73$ ) and for those present only in SV1 cells ( $4.15 \pm 0.69$ )  
200 but not for those present in both cell types.

201 2.8. Predicted pathogenicity scores of rare mutations of mitochondrial tRNA genes tend to be lower in SV1 cells  
202 than in SV22 cells.

203 Variants in mt-tRNA genes are a common cause of mitochondrial disease [29]. Thus, we  
204 calculated pathogenicity values for rare and subclonal mutations in mt-tRNA genes using the  
205 mitochondrial tRNA informatics predictor (MitoTIP) program of MITOMAP [29]. MitoTIP provides  
206 a raw score, which is derived from three sub-scores: variant history and conservation score, position  
207 score, and secondary structure score. A higher score represents a higher probability of  
208 pathogenicity.

209 We compared the raw pathogenicity values for rare and subclonal mutations in each of 22  
210 mt-tRNA genes found specifically in SV22 cells vs in SV1 cells. Eighty-three rare mutations were  
211 found in SV22 cells only; while 31 rare mutations were present in SV1 cells only. The exact same  
212 mutations specific to each cell type were observed in the subclonal range. The average pathogenicity  
213 score of mt-tRNA mutations tends to be lower in SV1 cells than in SV22 cells (Fig 5;  $p = 0.082$ ). In  
214 addition, we found four known/confirmed pathogenic tRNA variants (m.5650 G>A, m.5521 G>A,  
215 m.5690 A>G, m. 1630 A>G) among the 83 variants in SV22 cells, whereas confirmed pathogenic  
216 tRNA variants were not found in SV1 cells.



217

218 **Figure 5.** Predicted pathogenicity of rare unique mutations of mt-tRNAs. Predicted pathogenicity  
219 scores of rare variants in mt-tRNAs were obtained using MitoTIP and then were totaled for each  
220 region of tRNAs. Only the mutations present exclusively in each sample (mt-tRNA mutations  
221 present only in SV22 cells vs mt-tRNA mutations present only in SV1 cells) were included. The sums  
222 of predicted pathogenicity scores from each mt-tRNA region were averaged. Error bars represent the  
223 standard error of the mean (SEM).

224 2.9. Duplex Sequencing identifies many rare or subclonal mutations that are specific to SV22 and to SV1 cells.

225 To compare positions of mutations between SV22 and SV1 cells, only genome positions that  
226 had DCS read counts at least 100 or higher in both cell types were considered. Mutations occurring

227 at the same genome positions were scored only once and are referred to as unique mutations. We  
228 have identified rare and subclonal unique mutations that are present only in SV22 cells, only in SV1  
229 cells, or in both cell types.

230 A total of 792 rare and 797 subclonal mutations were found in SV22 cells only (but not in SV1  
231 cells); 527 rare and 528 subclonal mutations were found in SV1 cells only (but not in SV22 cells)  
232 (Table S4). 447 rare mutations were found in both SV22 and SV1 cells, of which 88 are more  
233 prevalent in SV22 than in SV1 and 9 are more prevalent in SV1 than in SV22 (prevalence meaning  
234 by at least a 3-fold difference) (Table S4). Similarly, 459 subclonal mutations were found in both  
235 SV22 and SV1 cells, of which 92 are more prevalent in SV22 than in SV1 and 11 are more prevalent  
236 in SV1 than in SV22 by at least a 3-fold difference (Table S4).

237 A detailed list of subclonal unique mutations, in which variant reads are at least two or greater,  
238 is presented in Table S5. Mutations were considered singlets if they have a variant read of 1, and  
239 these were excluded in Table S5. A total of 190 non-singlet subclonal mutations were observed only  
240 in SV22 cells but not in SV1 cells, whereas 122 non-singlet subclonal mutations were observed only  
241 in SV1 cells but not in SV22 cells (Table S5A, S5B). Among the identified subclonal mutations  
242 present in both SV22 and SV1 cells, 92 subclonal mutations were more highly mutated in SV22 cells  
243 than in SV1 cells by at least 3-fold (Table S5C). In contrast, only 11 subclonal mutations were more  
244 highly mutated in SV1 cells than in SV22 cells by at least 3-fold (Table S5D).

#### 245 *2.10. Independent DNA library preparation experiments of Duplex Sequencing produce reproducible results.*

246 Two independent DNA library preparation experiments were performed for SV1 cells.  
247 Consistent results of frequencies (Fig S4A), types (%) (Fig S4B), and sequence context spectra (%) of  
248 rare mutations (Fig S4C-D) were obtained from the two independent experiments. This validates the  
249 reproducibility of our Duplex Sequencing data.

### 250 **3. Discussion**

251 Ince et al (2007) reported that transformation of different normal human breast epithelial cell  
252 types led to distinct neoplastic phenotypes. This finding aligns with that the same oncogenes can  
253 have quite different phenotypic consequences depending on the cell origin [30,31]. Taken together,  
254 these suggest that the pre-existing differences in originator normal cell types significantly influence  
255 phenotypes of their transformed cells. Gordon et al (2014) demonstrated that immortalization of  
256 human fetal lung fibroblasts increased DNA methylation at gene promoters and caused large-scale  
257 changes in gene expression. While these studies [4,32] have examined tumorigenicity,  
258 histopathology, and metastatic behavior of human breast transformed cells or DNA methylation  
259 and gene expression of immortalized human fibroblasts, no study has examined the subclonal  
260 mutations of the whole mitochondrial genome for immortalized derivatives of phenotypically  
261 different normal cells.

262 In the current study, using Duplex Sequencing, we systemically examined both subclonal and  
263 clonal mutations of the whole mitochondrial genome for two types of immortalized HBECs [SV22  
264 (non-stem) vs SV1 (stem)]. Our data indicate that both rare and subclonal mutation frequencies are  
265 significantly lower in SV1 cells than in SV22 cells (Figs 1, S2). Previously, we compared rare  
266 mutations of the whole mitochondrial genome between paired normal HBECs (non-stem vs stem  
267 cells) from three independent women and we observed that normal stem cells from two women  
268 exhibited significantly lower frequencies of rare mutations than the matching non-stem cells [22].  
269 Our previous [22] and current findings suggest that the significantly low frequencies of rare and  
270 subclonal mutations of the whole mitochondria genome in stem cell-derived immortalized (SV1)  
271 cells can be attributed to mitochondrial mutations of their parental originator normal cell types. It  
272 supports the idea that distinct normal breast epithelial cell types lead to different mitochondrial  
273 mutagenesis in their immortalized/transformed cells.

274 Mechanisms for the lower frequencies of subclonal mutations in stem cell-derived  
275 immortalized cells (SV1) (Fig S2B) than in non-stem cell-derived immortalized cells (SV22) are  
276 unclear. A possible mechanism might be associated with lower levels of reactive oxygen species

277 (ROS). The lower ROS levels in stem cells could lead to reduced mtDNA damage and accumulation  
278 of subclonal mutations [33,34]. Stem cells might have more efficient systems of DNA repair and  
279 mitophagy for removing damaged mtDNA, therefore, lowering the number of mtDNA mutations  
280 generated [34-36]. These lower ROS levels and reduced mtDNA mutations of normal stem cells  
281 could be continually passed down to their immortalized cells.

282 Our results indicate that rare mutations are more prevalent in the non-coding RNA (ncRNA)  
283 regions (mt-RNR1; mt-RNR2; mt-tRNAs) than in the protein coding and control regions (Fig 3).  
284 Furthermore, the largest decrease in rare mutation burden in SV1 cells than in SV22 cells is  
285 observed in the ncRNA region (Fig 3). In ncRNA regions, the pathogenicity of mt-tRNA mutations  
286 can be predicted using the analysis tool MitoTIP (Fig 5). Our results indicate that the lower rare  
287 mutation burden of ncRNA genes in SV1 cells is accompanied by lower predicted pathogenicity of  
288 mt-tRNA mutations.

289 Furthermore, we demonstrate that four known pathological mt-tRNA gene mutations, m.5650  
290 G>A (mt-tRNAAla) [37], m.5521 G>A (mt-tRNATrp) [38], m.5690 A>G (mt-tRNAAsn) [39], and  
291 m.1630 A>G (mt-tRNAVal) [40,41] were present in SV22 cells. However, no known pathogenic  
292 mutations were found in the mt-tRNA genes of SV1 cells. Pathogenicities of these four mt-tRNA  
293 mutations were confirmed by several studies [37-41]. All four confirmed pathogenic mutations are  
294 related to causing myopathy, a common mitochondrial disease effectuated by impacting protein  
295 translation or affecting tRNA stability [37-41]. Cytochrome c oxidase (COX)-deficiency was  
296 commonly reported with all four mutations [37-41]. The m.5650 G>A mutation causes a phenotype  
297 of pure myopathy [37] and disrupts interaction between mitochondrial alanyl-tRNA synthetase and  
298 the mt-tRNAAla aminoacyl acceptor stem. The m.5521 G>A mutation may impact protein  
299 translation [38]. The m.5690 A>G mutation manifests in clinical presentations of chronic progressive  
300 external ophthalmoplegia and ptosis [39]. The m.1630 A>G mutation impairs oxygen consumption,  
301 which affects the stability of mt-tRNAVal and reduces the levels of subunits of the electron  
302 transport chain [41]. Horvath et al (2009) reported that the m.1630 A>G mutation may cause  
303 mitochondrial neurogastrointestinal encephalomyopathy such as gastrointestinal dysmotility and  
304 cachexia [40].

305 In human breast cancer, tRNA mutations can cause significant consequences due to their  
306 important roles in protein translation [42]. Mt-tRNA point mutations are typically caused by the  
307 loss of mt-tRNA stability, which leads to defective mitochondrial translation and respiratory chain  
308 deficiency [39] through: aberrant processing of mRNA transcripts by RNases P and ZL, impaired  
309 post-transcriptional mt-tRNA modification such as specific base modifications, 3-end additions of  
310 -CCA sequence and mt-tRNA aminoacylation, as well as compromised interaction of mt-tRNA with  
311 both mtEF-Tu (mitochondrial elongation factor Tu) and the mitoribosome [43]. Our results suggest  
312 that stem cell-derived immortalized (SV1) cells might possess a more stable mitochondrial genome,  
313 exhibited by lower subclonal mutation burden and lower predicted pathogenicity than non-stem  
314 cell-derived immortalized (SV22) cells.

315 In summary, we examined whether different phenotypes of originator normal human breast  
316 epithelial cells (non-stem vs stem) can lead to different profiles of mitochondrial mutations for their  
317 immortalized derivatives. Our results indicate that the vast majority of mutations in the cells are  
318 rarely occurring mutations, which are not detectable by conventional DNA sequencing methods,  
319 but are accurately detectable by Duplex Sequencing. The most prevalent rare mutation types are  
320 C>T/G>A and A>G/T>C transitions. Immortalized stem cells (SV1) exhibit lower frequencies of rare  
321 mutations than immortalized non-stem cells (SV22). The reduced mitochondrial rare mutation  
322 burden of immortalized stem cells mainly occurs in ncRNA regions of the whole mtDNA, and these  
323 are accompanied by reduced predicted pathogenicity. Our findings suggest that phenotypes of  
324 originator parental normal cells significantly influence and direct mutational profiles of the whole  
325 mitochondrial genome in their immortalized derivatives. Our results have implications in  
326 investigating genetic changes of mitochondrial genomes acquired during cellular immortalization  
327 and in characterizing immortalized stem (vs non-stem) cells, which represent in vitro preneoplastic  
328 stages of breast carcinogenesis.



## 329 4. Materials and Methods

### 330 4.1. Development and culture of immortalized human breast epithelial cells.

331 Immortalized cells (M13SV22, M13SV1) were derived from paired groups (non-stem vs stem)  
332 of normal human breast epithelial cells (HBECs) treated with SV40 large T-antigen (SV40-T).  
333 M13SV22 cells were derived from normal HBECs without stem cell features; M13SV1 cells were  
334 derived from normal HBECs with stem cell features. These immortalized cells were provided by  
335 Dr. Chia-Cheng Chang at Michigan State University (MSU) in East Lansing, MI, USA. A Material  
336 Transfer Agreement was approved by both MSU and University of Washington (UW).  
337 Development, characterization, and culture of normal HBEC and in vitro transformed HBECs were  
338 described previously [7,9-12,22,44-48].

339 4.2. DNA extraction, adapter synthesis, and DNA library preparation for Duplex Sequencing (DS) were  
340 carried out as we had described previously [22].

### 341 4.3. Data processing.

342 DS data were processed as described previously [16,17,22,49] with modifications. Previously,  
343 our in-house DS script processed and aligned two sequence read files of pair-end sequencing  
344 separately and independently before merging the two read files. For the current study, the script  
345 was modified to merge two sequence read files first then to process and align the merged file. This  
346 modification improved accuracy and efficiency of data processing. Sequence reads were aligned to  
347 the revised Cambridge Reference sequence (rCRS) reference genome (NC\_012920) using BWA and  
348 the genome analysis toolkit (GATK) software as described previously [22]. BWA “mem” was used  
349 in replacement of BWA “aln”. During processing, all datasets’ reads were filtered using a mapping  
350 quality score of 40. Pileup-based variant calling used the default base quality score of 13. The first  
351 four bases at 5’ and 3’ ends of each sequence reads were clipped to eliminate potential artifactual  
352 variants commonly present at the ends of each read.

353 4.4. Data analysis for positions, frequencies, types, and context spectra of mutations and annotation of genetic  
354 variants.

355 Genome positions with a DCS sequence read depth of 100 or greater were included for the data  
356 analysis. In addition, for comparing the mutations of SV22 and SV1 cells, only genome positions  
357 that had a minimum DCS read of 100 in matching positions of both samples were considered. The  
358 total number of DCS variant reads were divided by total number of DCS sequenced reads to  
359 calculate mutation frequencies for each sample. The total number of unique mutations (i.e. mutants  
360 were scored only once at each position of the genome regardless of number of variant reads  
361 observed in that position) were used for all other analyses, which includes fractions (%) of mutation  
362 types, mutation context spectra (%), and comparison of mutation positions. Genetic variant data  
363 from DS were annotated using Annotate Variation (ANNOVAR) bioinformatical software version  
364 2017Jun01 ([annovar.openbioinformatics.org](http://annovar.openbioinformatics.org)) [50]. Annotations were added for each sequenced  
365 position of the whole mitochondrial genome.

### 366 4.5. Predicted pathogenicity.

367 The MutPred program version 2.0 (<http://mutpred.mutdb.org>) [28] was performed to obtain  
368 pathogenicity scores of missense mutations in mt-protein coding regions as described previously  
369 [28,48]. The predicted pathogenicity scores for mt-tRNA mutations were analyzed using MitoTIP  
370 (August 2017 version) available *via* MITOMAP ([www.mitomap.org](http://www.mitomap.org)). MitoTIP analysis [29] involves  
371 calculating pathogenicity scores for each possible variant through a summation of variant history,  
372 conservation score, position score, and secondary structure score. Using publicly available  
373 databases, an algorithm that estimates the importance of a position across mtDNA was generated

374 and used in scoring. Pathogenicity scores ranged from -5.9 to 21.8 and were assigned to each  
375 variant in mt-tRNAs by its position.

#### 376 4.6. Statistical analysis.

377 Differences in mtDNA mutation frequencies and in the fraction (%) of mutation types between  
378 the two groups were analyzed by performing the prop.test for '2-sample equality of proportions  
379 with continuity correction' using an R program (version 3.4.4). To compare the MitoTIP predicted  
380 pathogenicity scores between the two groups, the Mann-Whitney U-test (Wilcoxon Rank-Sum test)  
381 was applied using Sigma Plot (version 12.0) (Systat Software, San Jose, CA). Differences between the  
382 two groups were considered significant if the p-value was less than 0.05.

383 **Supplementary Materials:** are available on line.

384 **Author Contributions:** Conceptualization, EHA; Data curation, EHA, SK, SSK, HEN, Formal analysis, SK, SSK,  
385 HEN, EHA; Funding acquisition, EHA; Investigation, EHA, SK, SSK, HEN; Methodology, EHA, HEN, SK;  
386 Project administration, EHA; Resources, EHA, SK, HEN; Software, HEN, SK; Supervision, EHA; Validation,  
387 EHA, SK, SSK, HEN; Visualization, SK, SSK, EHA, HEN; Writing - original draft, EHA; Writing - review &  
388 editing, EHA, HEN, SK, SSK.

389 **Funding:** The research was supported by grants from the National Institute of Environmental Health Sciences  
390 (NIEHS) P30 ES007033 sponsored-University of Washington (UW) Center for Exposures, Diseases, Genomics  
391 and Environment (EDGE) pilot grant (to EH Ahn), UW Office of Research Royalty Research Fund (to EH Ahn),  
392 and National Cancer Institute (NCI) P30 CA015704-39 Fred Hutchinson Cancer Research Center-UW Cancer  
393 Consortium Support Grant (to EH Ahn), NCI R21 CA220111 (to EH Ahn), and NCI of the National Institutes of  
394 Health (NIH) under award numbers P01 AG001751 and R33 CA181771 (to Lawrence A. Loeb). The content is  
395 solely the responsibility of the authors and does not necessarily represent the official views of the NIH.

396 **Acknowledgments:** We thank Drs. Chia-Cheng Chang, Brad L. Upham, and James E. Trosko for obtaining  
397 immortalized human breast epithelial cells and Seung Hyuk (Tony) Lee for editing the manuscript.

398 **Conflicts of Interest:** The authors declare no conflict of interest.

#### 399 Abbreviations

DCS	Duplex Consensus Sequence
DS	Duplex Sequencing
Mt	Mitochondrial
SV1	Normal stem cell-derived immortalized human breast epithelial cells (HBECs);
SV22	Normal non-stem cell-derived immortalized HBECs

#### 400 References

- 401 1. Böcker, W.; Moll, R.; Poremba, C.; Holland, R.; Van Diest, P.J.; Dervan, P.; Bürger, H.; Wai, D.; Ina Diallo,  
402 R.; Brandt, B.; et al. Common adult stem cells in the human breast give rise to glandular and myoepithelial  
403 cell lineages: a new cell biological concept. *Lab. Invest.* **2002**, *82*, 737–746.
- 404 2. Dontu, G.; Al-Hajj, M.; Abdallah, W.M.; Clarke, M.F.; Wicha, M.S. Stem cells in normal breast  
405 development and breast cancer. *Cell Prolif.* **2003**, *36 Suppl 1*, 59–72.
- 406 3. Welm, B.; Behbod, F.; Goodell, M.A.; Rosen, J.M. Isolation and characterization of functional mammary  
407 gland stem cells. *Cell Prolif.* **2003**, *36 Suppl 1*, 17–32.
- 408 4. Ince, T.A.; Richardson, A.L.; Bell, G.W.; Saitoh, M.; Godar, S.; Karnoub, A.E.; Iglehart, J.D.; Weinberg, R.A.  
409 Transformation of different human breast epithelial cell types leads to distinct tumor phenotypes. *Cancer*  
410 *Cell* **2007**, *12*, 160–170.
- 411 5. Keller, P.J.; Arendt, L.M.; Skibinski, A.; Logvinenko, T.; Klebba, I.; Dong, S.; Smith, A.E.; Prat, A.; Perou,  
412 C.M.; Gilmore, H.; et al. Defining the cellular precursors to human breast cancer. *Proc. Natl. Acad. Sci.*  
413 *U.S.A.* **2012**, *109*, 2772–2777.
- 414 6. Bu, W.; Liu, Z.; Jiang, W.; Nagi, C.; Huang, S.; Edwards, D.P.; Jo, E.; Mo, Q.; Creighton, C.J.; Hilsenbeck,  
415 S.G.; et al. Mammary Precancerous Stem and Non-Stem Cells Evolve into Cancers of Distinct Subtypes.  
416 *Cancer Res.* **2019**, *79*, 61–71.

- 417 7. Tai, M.-H.; Chang, C.-C.; Kiupel, M.; Webster, J.D.; Olson, L.K.; Trosko, J.E. Oct4 expression in adult  
418 human stem cells: evidence in support of the stem cell theory of carcinogenesis. *Carcinogenesis* **2005**, *26*,  
419 495–502.
- 420 8. Kang, K.S.; Morita, I.; Cruz, A.; Jeon, Y.J.; Trosko, J.E.; Chang, C.C. Expression of estrogen receptors in a  
421 normal human breast epithelial cell type with luminal and stem cell characteristics and its neoplastically  
422 transformed cell lines. *Carcinogenesis* **1997**, *18*, 251–257.
- 423 9. Kao, C.Y.; Nomata, K.; Oakley, C.S.; Welsch, C.W.; Chang, C.C. Two types of normal human breast  
424 epithelial cells derived from reduction mammoplasty: phenotypic characterization and response to SV40  
425 transfection. *Carcinogenesis* **1995**, *16*, 531–538.
- 426 10. Kao, C.-Y.; Oakley, C.S.; Welsch, C.W.; Chang, C.-C. Growth requirements and neoplastic transformation  
427 of two types of normal human breast epithelial cells derived from reduction mammoplasty. *In Vitro*  
428 *Cellular & Developmental Biology - Animal* **1997**, *33*, 282–288.
- 429 11. Chang, C.C.; Sun, W.; Cruz, A.; Saitoh, M.; Tai, M.H.; Trosko, J.E. A human breast epithelial cell type with  
430 stem cell characteristics as target cells for carcinogenesis. *Radiat. Res.* **2001**, *155*, 201–207.
- 431 12. Ahn, E.H.; Chang, C.-C.; Schroeder, J.J. Evaluation of sphinganine and sphingosine as human breast  
432 cancer chemotherapeutic and chemopreventive agents. *Exp. Biol. Med. (Maywood)* **2006**, *231*, 1664–1672.
- 433 13. Ahuja, D.; Sáenz-Robles, M.T.; Pipas, J.M. SV40 large T antigen targets multiple cellular pathways to elicit  
434 cellular transformation. *Oncogene* **2005**, *24*, 7729–7745.
- 435 14. Pipas, J.M. SV40: Cell transformation and tumorigenesis. *Virology* **2009**, *384*, 294–303.
- 436 15. Sun, W.; Kang, K.S.; Morita, I.; Trosko, J.E.; Chang, C.C. High susceptibility of a human breast epithelial  
437 cell type with stem cell characteristics to telomerase activation and immortalization. *Cancer Res.* **1999**, *59*,  
438 6118–6123.
- 439 16. Schmitt, M.W.; Kennedy, S.R.; Salk, J.J.; Fox, E.J.; Hiatt, J.B.; Loeb, L.A. Detection of ultra-rare mutations by  
440 next-generation sequencing. *Proc. Natl. Acad. Sci. U.S.A.* **2012**, *109*, 14508–14513.
- 441 17. Kennedy, S.R.; Schmitt, M.W.; Fox, E.J.; Kohrn, B.F.; Salk, J.J.; Ahn, E.H.; Prindle, M.J.; Kuong, K.J.; Shen,  
442 J.-C.; Risques, R.-A.; et al. Detecting ultralow-frequency mutations by Duplex Sequencing. *Nat Protoc* **2014**,  
443 *9*, 2586–2606.
- 444 18. Schmitt, M.W.; Fox, E.J.; Prindle, M.J.; Reid-Bayliss, K.S.; True, L.D.; Radich, J.P.; Loeb, L.A. Sequencing  
445 small genomic targets with high efficiency and extreme accuracy. *Nat. Methods* **2015**, *12*, 423–425.
- 446 19. Ahn, E.H.; Lee, S.H. Detection of Low-Frequency Mutations and Identification of Heat-Induced  
447 Artifactual Mutations Using Duplex Sequencing. *Int J Mol Sci* **2019**, *20*.
- 448 20. Lou, D.I.; Hussmann, J.A.; McBee, R.M.; Acevedo, A.; Andino, R.; Press, W.H.; Sawyer, S.L.  
449 High-throughput DNA sequencing errors are reduced by orders of magnitude using circle sequencing.  
450 *Proc. Natl. Acad. Sci. U.S.A.* **2013**, *110*, 19872–19877.
- 451 21. Fox, E.J.; Reid-Bayliss, K.S.; Emond, M.J.; Loeb, L.A. Accuracy of Next Generation Sequencing Platforms.  
452 *Next Gener Seq Appl* **2014**, *1*.
- 453 22. Ahn, E.H.; Hirohata, K.; Kohrn, B.F.; Fox, E.J.; Chang, C.-C.; Loeb, L.A. Detection of Ultra-Rare  
454 Mitochondrial Mutations in Breast Stem Cells by Duplex Sequencing. *PLoS ONE* **2015**, *10*, e0136216.
- 455 23. Taylor, R.W.; Turnbull, D.M. Mitochondrial DNA mutations in human disease. *Nat. Rev. Genet.* **2005**, *6*,  
456 389–402.
- 457 24. Chan, D.C. Mitochondria: dynamic organelles in disease, aging, and development. *Cell* **2006**, *125*,  
458 1241–1252.
- 459 25. Salk, J.J.; Schmitt, M.W.; Loeb, L.A. Enhancing the accuracy of next-generation sequencing for detecting  
460 rare and subclonal mutations. *Nat. Rev. Genet.* **2018**, *19*, 269–285.
- 461 26. Strachan, T.; Read, A.P. *Human molecular genetics*; 2nd ed.; Wiley: New York, 1999; ISBN 978-0-471-33061-5.
- 462 27. Govatati, S.; Deenadayal, M.; Shivaji, S.; Bhanoori, M. Mitochondrial displacement loop alterations are  
463 associated with endometriosis. *Fertil. Steril.* **2013**, *99*, 1980-1986.e9.
- 464 28. Pejaver, V.; Urresti, J.; Lugo-Martinez, J.; Pagel, K.A.; Lin, G.N.; Nam, H.-J.; Mort, M.; Cooper, D.N.; Sebat,  
465 J.; Iakoucheva, L.M.; et al. MutPred2: inferring the molecular and phenotypic impact of amino acid  
466 variants. *bioRxiv* **2017**.
- 467 29. Sonney, S.; Leipzig, J.; Lott, M.T.; Zhang, S.; Procaccio, V.; Wallace, D.C.; Sondheimer, N. Predicting the  
468 pathogenicity of novel variants in mitochondrial tRNA with MitoTIP. *PLoS Comput. Biol.* **2017**, *13*,  
469 e1005867.
- 470 30. Vogelstein, B.; Kinzler, K.W. Cancer genes and the pathways they control. *Nat. Med.* **2004**, *10*, 789–799.

- 471 31. Gupta, G.P.; Massagué, J. Cancer metastasis: building a framework. *Cell* **2006**, *127*, 679–695.
- 472 32. Gordon, K.; Clouaire, T.; Bao, X.X.; Kemp, S.E.; Xenophontos, M.; de Las Heras, J.I.; Stancheva, I.  
473 Immortality, but not oncogenic transformation, of primary human cells leads to epigenetic  
474 reprogramming of DNA methylation and gene expression. *Nucleic Acids Res.* **2014**, *42*, 3529–3541.
- 475 33. Saretzki, G.; Walter, T.; Atkinson, S.; Passos, J.F.; Bareth, B.; Keith, W.N.; Stewart, R.; Hoare, S.; Stojkovic,  
476 M.; Armstrong, L.; et al. Downregulation of multiple stress defense mechanisms during differentiation of  
477 human embryonic stem cells. *Stem Cells* **2008**, *26*, 455–464.
- 478 34. Frosina, G. The bright and the dark sides of DNA repair in stem cells. *J. Biomed. Biotechnol.* **2010**, *2010*,  
479 845396.
- 480 35. Guan, J.-L.; Simon, A.K.; Prescott, M.; Menendez, J.A.; Liu, F.; Wang, F.; Wang, C.; Wolvetang, E.;  
481 Vazquez-Martin, A.; Zhang, J. Autophagy in stem cells. *Autophagy* **2013**, *9*, 830–849.
- 482 36. Joshi, A.; Kundu, M. Mitophagy in hematopoietic stem cells: the case for exploration. *Autophagy* **2013**, *9*,  
483 1737–1749.
- 484 37. McFarland, R.; Swalwell, H.; Blakely, E.L.; He, L.; Groen, E.J.; Turnbull, D.M.; Bushby, K.M.; Taylor, R.W.  
485 The m.5650G>A mitochondrial tRNA<sup>Ala</sup> mutation is pathogenic and causes a phenotype of pure  
486 myopathy. *Neuromuscul. Disord.* **2008**, *18*, 63–67.
- 487 38. Porcelli, A.M.; Ghelli, A.; Ceccarelli, C.; Lang, M.; Cenacchi, G.; Capristo, M.; Pennisi, L.F.; Morra, I.;  
488 Ciccarelli, E.; Melcarne, A.; et al. The genetic and metabolic signature of oncocytic transformation  
489 implicates HIF1 $\alpha$  destabilization. *Hum. Mol. Genet.* **2010**, *19*, 1019–1032.
- 490 39. Blakely, E.L.; Yarham, J.W.; Alston, C.L.; Craig, K.; Poulton, J.; Brierley, C.; Park, S.-M.; Dean, A.; Xuereb,  
491 J.H.; Anderson, K.N.; et al. Pathogenic mitochondrial tRNA point mutations: nine novel mutations affirm  
492 their importance as a cause of mitochondrial disease. *Hum. Mutat.* **2013**, *34*, 1260–1268.
- 493 40. Horváth, R.; Bender, A.; Abicht, A.; Holinski-Feder, E.; Czermin, B.; Trips, T.; Schneiderat, P.; Lochmüller,  
494 H.; Klopstock, T. Heteroplasmic mutation in the anticodon-stem of mitochondrial tRNA(Val) causing  
495 MNGIE-like gastrointestinal dysmotility and cachexia. *J. Neurol.* **2009**, *256*, 810–815.
- 496 41. Glatz, C.; D'Aco, K.; Smith, S.; Sondheimer, N. Mutation in the mitochondrial tRNA(Val) causes  
497 mitochondrial encephalopathy, lactic acidosis and stroke-like episodes. *Mitochondrion* **2011**, *11*, 615–619.
- 498 42. Meng, X.-L.; Meng, H.; Zhang, W.; Qin, Y.-H.; Zhao, N.-M. The role of mitochondrial tRNA variants in  
499 female breast cancer. *Mitochondrial DNA A DNA Mapp Seq Anal* **2016**, *27*, 3199–3201.
- 500 43. Lvinger, L.; Oestreich, I.; Florentz, C.; Mörl, M. A pathogenesis-associated mutation in human  
501 mitochondrial tRNA<sup>Leu</sup>(UUR) leads to reduced 3'-end processing and CCA addition. *J. Mol. Biol.* **2004**,  
502 337, 535–544.
- 503 44. Kang, K.S.; Sun, W.; Nomata, K.; Morita, I.; Cruz, A.; Liu, C.J.; Trosko, J.E.; Chang, C.C. Involvement of  
504 tyrosine phosphorylation of p185(c-erbB2/neu) in tumorigenicity induced by X-rays and the neu oncogene  
505 in human breast epithelial cells. *Mol. Carcinog.* **1998**, *21*, 225–233.
- 506 45. Park, J.-S.; Noh, D.-Y.; Kim, S.-H.; Kim, S.-H.; Kong, G.; Chang, C.-C.; Lee, Y.-S.; Trosko, J.E.; Kang, K.-S.  
507 Gene expression analysis in SV40-immortalized human breast luminal epithelial cells with stem cell  
508 characteristics using a cDNA microarray. *Int. J. Oncol.* **2004**, *24*, 1545–1558.
- 509 46. Ahn, E.H.; Chang, C.-C.; Talmage, D.A. Loss of anti-proliferative effect of all-trans retinoic acid in  
510 advanced stage of breast carcinogenesis. *Anticancer Res.* **2009**, *29*, 2899–2904.
- 511 47. Wang, K.-H.; Kao, A.-P.; Chang, C.-C.; Lee, J.-N.; Hou, M.-F.; Long, C.-Y.; Chen, H.-S.; Tsai, E.-M.  
512 Increasing CD44<sup>+</sup>/CD24<sup>-</sup> tumor stem cells, and upregulation of COX-2 and HDAC6, as major functions  
513 of HER2 in breast tumorigenesis. *Mol. Cancer* **2010**, *9*, 288.
- 514 48. Ahn, E.H.; Lee, S.H.; Kim, J.Y.; Chang, C.-C.; Loeb, L.A. Decreased Mitochondrial Mutagenesis during  
515 Transformation of Human Breast Stem Cells into Tumorigenic Cells. *Cancer Res.* **2016**, *76*, 4569–4578.
- 516 49. Pickrell, A.M.; Huang, C.-H.; Kennedy, S.R.; Ordureau, A.; Sideris, D.P.; Hoekstra, J.G.; Harper, J.W.;  
517 Youle, R.J. Endogenous Parkin Preserves Dopaminergic Substantia Nigral Neurons following  
518 Mitochondrial DNA Mutagenic Stress. *Neuron* **2015**, *87*, 371–381.
- 519 50. Wang, K.; Li, M.; Hakonarson, H. ANNOVAR: functional annotation of genetic variants from  
520 high-throughput sequencing data. *Nucleic Acids Res.* **2010**, *38*, e164.
- 521